Zinc Is Required for FcεRI-Mediated Mast Cell Activation[1]

Koki Kabu,*† Satoru Yamasaki,* Daisuke Kamimura,* Yukitaka Ito,*† Aiko Hasegawa,*† Emi Sato,*† Hidemitsu Kitamura,* Keigo Nishida,* and Toshio Hirano[2]*†

Zinc (Zn) is an essential nutrient, and its deficiency causes growth retardation, immunodeficiency, and neuronal degeneration. However, the precise roles and molecular mechanism(s) of Zn function in immune response have not been clarified. Mast cells (MCs) are granulated cells that play a pivotal role in allergic reactions and inflammation. The granules of MCs contain various chemical mediators and inflammatory cytokines that are released upon FcεRI cross-linking. In this study, we report that Zn is essential for MC activation both in vitro and in vivo. We showed that a Zn chelator, *N,N,N,N*-tetrakis (2-pyridylmethyl) ethylenediamine, inhibited in vivo allergic reactions such as PCA and PSA. Consistent with this, *N,N,N,N*-tetrakis (2-pyridylmethyl) ethylenediamine significantly inhibited the FcεRI-induced degranulation and cytokine production. We found that Zn was required for FcεRI-induced translocation of granules to the plasma membrane, a process that we have shown to be important for MC degranulation. In addition, we showed that Zn was essential for plasma membrane translocation of protein kinase C and subsequent nuclear translocation of NF-κB, leading to cytokine production, such as IL-6 and TNF-α. These results revealed that Zn was involved in multiple steps of FcεRI-induced MC activation and required for degranulation and cytokine production. ***The Journal of Immunology,*** **2006, 177: 1296–1305.**

Zinc (Zn)[3] is an essential nutrient, and its deficiency causes growth retardation, immunodeficiency, and neuronal degeneration (1, 2). There are many enzymes, signaling molecules, and transcription factors whose function is critically dependent on and/or regulated by Zn. Electron microscopic studies in the 1960s demonstrated that mast cell (MC) granules are rich in Zn (3). However, the precise roles and molecular mechanism(s) of Zn function in MCs have not been clarified.

MCs are thought to participate in a variety of immune responses, such as allergic reaction, innate immunity, and autoimmunity (4–11). Engagement of the FcεRI on MCs initiates signaling pathways leading to the exocytosis of granules containing various cytokines and chemical mediators. These released molecules play pivotal roles in the inflammatory reactions observed in patients with allergy and autoimmune diseases.

The antigenic cross-linking of FcεRI induces the activation of several protein tyrosine kinases, resulting in elevated levels of inositol 1,4,5-trisphosphate and free intracellular calcium (12–15). The degranulation process is thought to be mediated by granule-to-plasma and granule-to-granule membrane fusion (16, 17). This membrane-fusion process is regulated by the Lyn/SLP-76, LAT/PLCγ1-calcium mobilization pathway. In addition to this calcium-dependent process, we recently showed that a calcium-independent process is required for microtubule-dependent granule translocation to the plasma membrane (18). This calcium-independent process is regulated by the Fyn/Gab2/RhoA signaling pathway, but not by Lyn/SLP-76 (18).

In contrast, FcεRI stimulation can induce the de novo synthesis of proinflmmatory cytokines such as IL-6 and TNF-α (19, 20). Especially both calcium and diacylglycerol activate conventional protein kinase C (cPKC) isoforms that mediate a critical positive signal necessary for cytokine production in MCs (21, 22). In addition, cPKCs have two common regions in the regulatory domain, C1 and C2. The C1 region has two cysteine-rich loops (Zn finger-like motifs) that interact with diacylglycerol or phorbol esters and regulate activation or translocation of PKC (23–25). The C2 region mediates calcium binding. Previous studies using PKCβ-deficient mice revealed that bone marrow-derived MCs (BMMCs) lacking both PKCβI and PKCβIII exhibited lower levels of IL-6 release than did the wild-type cells in response to Ag (26). Collectively, these reports indicate that PKC isoforms play important roles in cytokine production.

In this study, we found that Zn was required for both degranulation and cytokine production in MCs. In fact, Zn was essential for granule translocation to the plasma membrane. Furthermore, Zn was required for FcεRI-mediated plasma membrane translocation of PKC and NF-κB activation.

Materials and Methods

Metal chelators and Abs

N,N,N,N-tetrakis (2-pyridylmethyl) ethylenediamine) (TPEN) (K_a = $10^{15.58}$ M^{-1}, $10^{14.61}$ M^{-1}, 10^{10} M^{-1}, $10^{10.27}$ M^{-1} for Zn^{2+}, Fe^{2+}, Cu^{2+}, and Mn^{2+}, respectively) (27, 28); ZnAF-2DA (aminofluorescein-2 diacetate (K_a = $10^{9.15}$ M^{-1} for Zn^{2+}) (29, 30); 2,2′-dipyridyl (K_a = $10^{17.2}M^{-1}$ for Fe^{2+}); desferrioxamine mesylate (K_a = 10^{31} M^{-1} for Fe^{3+}) (31); disodium bathocuproine disulphonate (for Cu^{2+}) (31), and *p*-aminosalicylic acid (for Mn^{2+}) (32, 33). TPEN, 2,2′-dipyridyl, desferrioxamine, and bathocuproine disulphonate were all purchased from Sigma-Aldrich. Zn

*Laboratory for Cytokine Signaling, RIKEN Research Center for Allergy and Immunology (RCAI), Yokohama, Kanagawa, Japan; and †Laboratories of Developmental Immunology, Graduate School of Frontier Biosciences and Graduate School of Medicine, Osaka University, Osaka, Japan

Received for publication December 29, 2005. Accepted for publication April 21, 2006.

The costs of publication of this article were defrayed in part by the payment of page charges. This article must therefore be hereby marked *advertisement* in accordance with 18 U.S.C. Section 1734 solely to indicate this fact.

[1] This work was supported by grants from the Ministry of Education, Culture, Sports, Science, and Technology in Japan. K.K is a Junior Research Associate, Laboratory for Cytokine Signaling, RIKEN Research Center for Allergy and Immunology, Yokohama, Kanagawa, Japan.

[2] Address correspondence and reprint requests to Dr. Toshio Hirano, Laboratory of Developmental Immunology, Graduate School of Medicine C-7, Osaka University, 2-2, Yamada-oka, Suita, Osaka, 565-0871, Japan. E-mail address: hirano@molonc.med.osaka-u.ac.jp

[3] Abbreviations used in this paper: Zn, zinc; MC, mast cell; BMMC, bone marrow-derived MC; TPEN, *N,N,N,N*-tetrakis (2-pyridylmethyl) ethylenediamine; ZnAF-2DA, Zn aminofluorescein-2 diacetate; PCA, passive cutaneous anaphylaxis; PSA, passive systemic anaphylaxis; 7AAD, 7-aminoactinomycin D; PKC, protein kinase C; cPKC, conventional PKC; IKKα, β-IκB kinase αβ; PVDF, polyvinylidene difluoride.

Copyright © 2006 by The American Association of Immunologists, Inc.

0022-1767/06/$02.00

indicators, Newport green, and ZnAF-2DA were purchased from Molecular Probes and Dai-ichi Kagaku, respectively. Abs for Syk, p65, phospho-IKK$\alpha\beta$, IKK$\alpha\beta$, PKCβI, and Lyn were all purchased form Santa Cruz Biotechnology. Abs for LAT, PLCγ1, Gab2, pIκBα, and IκBα were purchased from Upstate Biotechnology, and anti-β-tubulin was from Sigma-Aldrich. Anti-Fyn mAb was a gift from K. Hattori (National Center of Neurology and Psychiatry, Tokyo, Japan).

Cell culture

BMMCs were prepared as described previously (34). Briefly, 8-wk-old C57/BL6 mice were sacrificed, and their BM cells were cultured in RPMI 1640 medium supplemented with 10% heat-inactivated FCS, 10 mU/ml penicillin, 0.1 mg/ml streptomycin, 40 μM 2-ME, and IL-3 in a 5% CO_2 and 95% humidified atmosphere at 37°C. After 4–5 wk of culture, the cells were confirmed to show the cell surface expression of FcεRI and c-*Kit* and were used for experiments (< 98% MCs).

BMMC degranulation assay

Cells (1×10^6/ml) were sensitized with 1 μg/ml IgE (anti-DNP IgE clone SPE-7; Sigma-Aldrich) for 6 h at 37°C. After sensitization, the cells were washed twice with Tyrode's buffer (10 mM HEPES (pH 7.4), 130 mM NaCl, 5 mM KCl, 1.4 mM $CaCl_2$, 1 mM $MgCl_2$, 5.6 mM glucose), then suspended in the same buffer containing 0.1% BSA and stimulated with polyvalent dinitrophenyl-human serum albumin (DNP-HSA; Sigma-Aldrich) for 30 min. For the β-hexosaminidase reaction, 50 μl of supernatant or cell lysate and 100 μl of 1.3 mg/ml *p*-nitrophenyl-*N*-acetyl-*d*-glucosamide (in 0.1 M citrate, pH 4.5) were added to each well of a 96-well plate, and the color was developed for 60 min at 37°C. The enzyme reaction was then stopped by adding 150 μl of 0.2 M glycine-NaOH (pH 10.2), and the absorbance at 405 nm was measured in a microplate reader (Bio-Rad). Cells were lysed with Tyrode's buffer containing 1% Triton X-100, and the β-hexosaminidase activity was measured. The percentage of β-hexosaminidase released was calculated using the following formula: percentage release = supernatant/(supernatant + cell lysate) × 100.

Measurement of cytokines and chemical mediators

Cells were activated as described above, and TNF-α and IL-6 in the cell culture supernatants were measured with an ELISA kit (BioSource International). Histamine and leukotrienes were determined using an ELISA kit (Beckman Coulter and Cayman Chemical, respectively), following the manufacturer's recommendation.

Cell lysates and immunoblotting.

BMMCs (1×10^6/ml) were sensitized with 1 μg/ml IgE for 6 h at 37°C. Cells were either untreated or treated with 10 μM TPEN for 2 h, then stimulated with 100 ng/ml DNP-HSA for 0, 2, 5, 15, or 30 min. After stimulation, the cells were harvested and lysed with 100 μl of lysis buffer (20 mM Tris-HCl (pH 7.4) 4°C, 150 mM NaCl, 1% Nonidet P-40, 0.1% SDS, 0.1% deoxycholate, 1 mM $NaVO_4$, 3 mM EDTA, and proteinase inhibitors, (0.5 mM PMSF), 10 μg/ml aprotinin, 5 μg/ml pepstatin, 10 μg/ml leupeptin)) for 30 min at 4°C and spun at 12,000 × *g*, 4°C, for 15 min. The eluted and reduced samples were resolved by SDS-PAGE using a 4–20% gradient polyacrylamide gel (Dai-ichi Kagaku) and transferred to a polyvinylidene difluoride (PVDF) membrane (Immobilon-P; Millipore). For immunoblotting, membranes were incubated with anti-p65, anti-phospho IκBα, anti-IκBα, anti-β-tubulin, anti-phospho-IKK$\alpha\beta$, anti-IKK$\alpha\beta$, anti-PKCβI, and anti-Lyn, respectively. For immunoprecipitation, the cell lysates were incubated for 4 h at 4°C with 1 μg of Abs bound to protein A Sepharose. The eluted and reduced samples were separated on a 4–20% gradient SDS-polyacrylamide gel and transferred to a PVDF membrane. The membranes were incubated with anti-phosphotyrosine. Following first Ab blotting, the membranes were blotted with HRP-conjugated species-specific mouse-anti-IgG (Zymed) for 1 h at room temperature. After extensive washing of the membranes, immunoreactive proteins were visualized using the Renaissance chemiluminescence system (NEN) according to the manufacturer's recommendation. The PVDF membranes were exposed to Fuji RX film. As for phospho-IKKβ and PKCβI, densitometrical analysis was performed by LAS-1000 (Fuji).

Preparation of nuclear protein and plasma membrane protein

Nuclear protein was prepared as mentioned elsewhere. Briefly, BMMCs (1×10^6/ml) were sensitized with 1 μg/ml IgE for 6 h at 37°C. After sensitization, Ag-stimulated 5×10^6 cells were washed by ice-cold PBS $^-$ (PBS without calcium and magnesium) and suspended in 400 μl of ice-cold hypotonic buffer [10 mM HEPES-KOH (pH 7.8), 10 mM KCl, 0.1 mM EDTA (pH 8.0), 0.1% Nonidet P-40, 1 mM DTT, and protein inhibitors (0.5 mM PMSF, 10 μg/ml aprotinin, 5 μg/ml pepstatin, 10 μg/ml leupeptin)]. To obtain the crude nuclear fractions, the suspensions were centrifuged at 2,500 × *g*, 4 °C for 1 min. The pellets were resuspended in hypertonic buffer [50 mM HEPES-KOH (pH 7.8), 420 mM KCl, 0.1 mM EDTA (pH 8.0), 5 mM $MgCl_2$, 20% glycerol, 1 mM DTT, and protein inhibitors (0.5 mM PMSF, 10 μg/ml aprotinin, 5 μg/ml pepstatin, 10 μg/ml leupeptin)] and centrifuged at 12,000 × *g*, 4°C for 15 min. The supernatants were applied for immunoblotting to detect p65. Plasma membrane proteins were extracted using the Plasma Membrane Protein Extraction Kit (BioVision; K268-50) according to the manufacturer's recommendation. The plasma membrane fractions were used for immunoblot to detect PKCβI.

Calcium influx measurement

BMMCs (1×10^6/ml) were sensitized with 1 μg/ml IgE for 12 h and incubated with the calcium-sensitive dye indo-1 AM (Molecular Probes) in the presence of F 127 and 0.2% FBS at 37°C for 30 min. The cells were washed twice and resuspended in 1 ml Tyrode's buffer containing 1 mM $CaCl_2$. Cells were analyzed for calcium mobilization in a BD-LSR flow cytometer (BD Bioscience). Values were plotted as the ratio of fluorescence at FL5 (Ca^{2+}-bound indo-1) to that at FL4 (Ca^{2+}-free indo-1).

Retroviral infection

Retroviral infection was performed as previously described. The CD63-GFP plasmid (a kind gift from M. Nakanishi, Nagoya City University) was inserted into the *Bam*HI and *Not*I sites of the retroviral vector pMX (a gift from T. Kitamura, University of Tokyo). This construct was then used to transfect the 293T-based packaging cell line, phoenix (a gift from G. Nolan, Stanford University, Stanford, CA), with Lipofectamine 2000 (Invitrogen Life Technologies) to generate recombinant retroviruses. BM cells were infected with the retrovirus in the presence of 10 μg/ml polybrene (Sigma-Aldrich) and IL-3.

Cell surface expression of CD63 upon Ag stimulation

BMMCs (1×10^6/ml) were sensitized with 1 μg/ml IgE for 6 h at 37°C. After Ag stimulation with 100 ng/ml DNP-HSA for 10 min, the cells were fixed with 4% paraformaldehyde (pH 7.4) for 30 min at room temperature. Cells were stained with 1 μl of anti-CD63 and then with PE-labeled anti-rat IgG (Cedarlane Laboratories). The exposure of CD63 to the cell surface was analyzed by flow cytometer (BD Biosciences).

Intracellular Zn measurement

BMMCs (2×10^6 cells) were treated with 5 μM Newport Green for 10 min under three conditions: no treatment, pretreatment with 10 μM TPEN, or pretreatment with 1 μM pyrithione plus 10 μM ZnSO4. The cells were washed two times with PBS (−) before fluorescent intensity was measured by FACS.

Confocal microscopy and granule translocation

Separate aliquots of 5×10^5 cells were each sensitized with 1 μg/ml IgE for 6 h. The cells were then stimulated with 100 ng/ml DNP-HSA for 10 min at 37°C and fixed with 4% paraformaldehyde for 30 min at 37°C. The cells were spun at 12,000 × *g* for 5 min and permeabilized in Perm Buffer (BD Biosciences) containing 1% BSA for 15 min at room temperature. The cells were washed with 1 ml of PBS (−) twice, then resuspended in 100 μl of PBS (−) and attached to glass slides by cytospin (Thramo Shandon) at 600 rpm for 6 min. Primary and secondary stainings were performed on the slides: anti-p65 at a dilution of 1/50, anti-PKCβI at a dilution of 1/50, anti-β-tubulin at a dilution of 1/50, FITC-conjugated anti-rabbit IgG, (Molecular Probes), FITC-conjugated anti-mouse IgG (Molecular Probes) at 1/50, and phalloidin-rhodamine (Molecular Probes) at 1/150. Confocal microscopy was conducted using the TCS SL system (Leica). The frequency of Ag-induced MC granule translocation was enumerated according to the following criteria: 1) the increase of yellow color fluorescence around plasma membrane, which was a result of the merge of phalloidin-rhodamine and CD63-GFP signal; and 2) the obvious decrease of the cytoplasmic area containing CD63-GFP, compared with that of nonstimulated cells. The cells that satisfied both criteria were considered to be positive for granule translocation. Two hundred independent GFP-positive cells were counted for each experiment. The data are representative of three independent experiments, and the values are the mean ± SEM.

RT-PCR and real-time quantitative RT-PCR analysis

Cells were homogenized with Sepasol RNAI (Nacalai Tesque), and total RNA was isolated according to manufacturer's instructions. For standard

RT-PCR, cDNA was synthesized from 500 ng of total RNA by incubating with reverse transcriptase (ReverTra Ace; Toyobo) and 500 ng of oligo (dT) primer for 30 min at 42 °C (Invitrogen Life Technologies). A portion of the cDNA (typically 1/20 volume) was used for standard PCR to detect IL-6, TNF-α, and GAPDH. Twenty-five cycles of PCR were performed with 0.5 U of rTaq DNA polymerase and 10 pmol of gene-specific sense and antisense primers. For real-time quantitative RT-PCR, IL-6, and TNF-α gene expression was measured relative to GAPDH using Syber Green (Applied Biosystem). Primers used in this experiments were purchased from Invitrogen Life Technologies, and sequences were as follows: IL-6, (forward) 5′-GAGGATACCACTCCCAACAGACC-3′ and (reverse) 5′-AAGTGCATCATCGTTGTTCATACA-3′; TNF-α, (forward) 5′-CATCTTCTCAAAATTCGAGTGACAA-3′ and (reverse) 5′-TGGGAG TAGACAAGGTACAACCC-3′; GAPDH, (forward) 5′-TTCACCAC CATGGAGAAGGCCG-3′ and (reverse) 5′-GGCATGGACTGTGGTC ATGA-3′. PCR product was separated on an agarose gel, stained with ethidium bromide (500 ng/ml), and photographed.

Passive cutaneous anaphylaxis (PCA) and histology of the ears.

A total of 0.5 μg of IgE was injected s.c. into both ears of BALB/c mice for 12 h or overnight. After sensitization, either vehicle or TPEN was injected into the mice i.p. at the concentration indicated for 30 min, and the mice were then challenged with an i.v. injection of 250 μg of polyvalent dinitrophenyl-BSA (DNP-BSA; Cosmobio) in 250 μl of saline-5 mg/ml Evans blue dye (Sigma-Aldrich). Extravasation of Evans blue in the ear was monitored for 30 min, then the mice were sacrificed, both ears were dissected, and the Evans blue dye was extracted in 700 μl of formamide at 63°C overnight. The absorbance of Evans blue-extracted formamide was then measured at 620 nm. To observe the ear MCs, 5-μm paraffin sections were fixed and stained with nuclear fast red and alcian blue. Approximately 100 alcian blue-stained cells in each sample were counted, and the ratio of morphologically degranulated MCs to total MCs was calculated. We obtained approval from the Animal Research Committee at RIKEN for all animal experiments performed.

Passive systemic anaphylaxis (PSA)

To determine the amount of histamine released in response to PSA, we sensitized mice by the i.v. injection with 0.5 μg of IgE for 12 h. After sensitization, mice were i.v. challenged with 30 μg of DNP-BSA. One minute after the Ag challenge, blood was drawn directly from the heart, and the plasma fraction was collected by centrifugation. The plasma histamine level was measured as described above.

Results

Zn chelator inhibits Ag-dependent PCA and PSA

To study potential roles for Zn in MC function, we assessed the efficacy of Zn chelator TPEN on in vivo allergic reactions involving normal tissue-resident MCs. We first tested the effect of TPEN in a mouse PCA model, in which Ag-specific IgE was injected into the ear. Pretreatment with the intraperitoneal administration of TPEN significantly inhibited the IgE-dependent PCA reactions (44.9, 75.7, and 87.4% inhibition by a single dose of TPEN at 10, 20, and 30 mg/kg, respectively) (Fig. 1, *A* and *B*). We then analyzed the MCs in the ear histologically. In sham-treated control mice, intact MCs densely filled with granules (blue) were easily identified (Fig. 1*C*, *left panel*), and degranulated MCs were detected as early as 30 min after Ag challenge (Fig. 1*C*, *right panel*). In contrast, the number of degranulated MCs was significantly

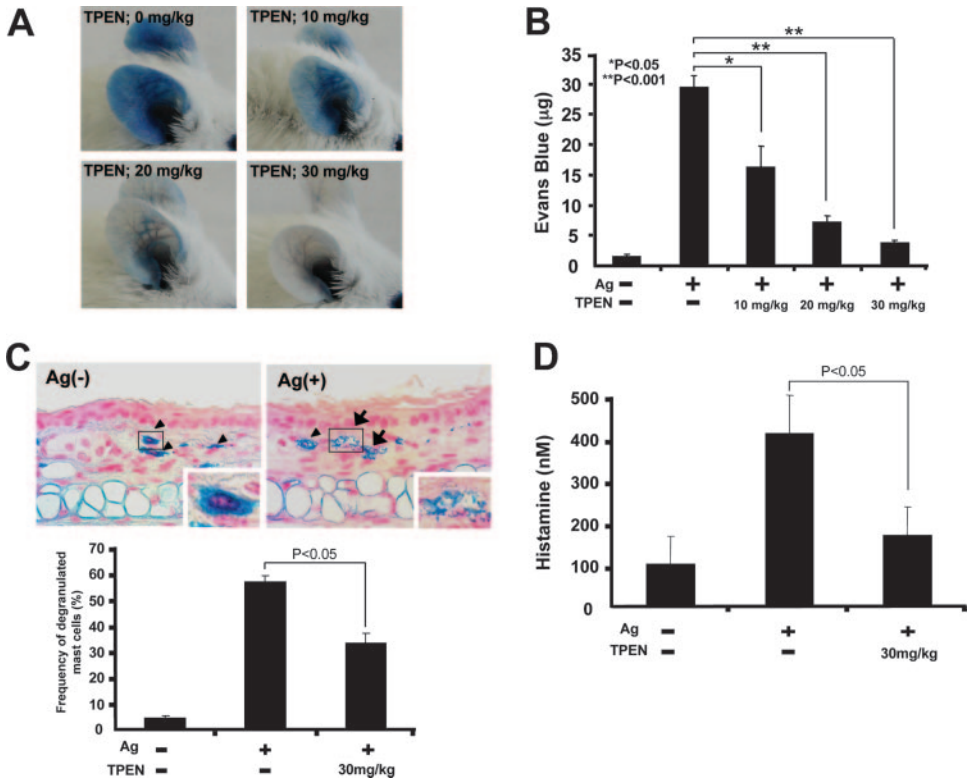

FIGURE 1. Zn chelator administration inhibits Ag-dependent PCA and PSA. *A*, The effects of TPEN on the PCA reaction were verified. Mice were sensitized with IgE injected into the ear, then challenged with 250 μg Ag and Evans Blue i.v. for 30 min. The injected Evans blue dye was extravasated into the ears of control mice (0 mg/kg, $n = 10$), but a dose-dependent inhibition was observed in TPEN-treated mice (10, 20, and 30 mg/kg, $n = 5$ respectively). Almost no Evans blue dye extravasation was observed in saline-challenged mice (data not shown). *B*, The amount of extravasated Evans Blue dye in both ears was calculated by extracting the dye and measuring the OD of the extract at 620 nm. *C*, *Upper*, Histological analysis of MCs in the ear. Ear sections were stained with nuclear fast red and alcian blue. Granules and the nucleus were stained blue and red respectively. Representative sections containing granulated MCs (*upper left*, arrowheads) and degranulated MCs (*upper right*, arrows) are shown. *Lower*, Approximately 100 cells in the sections were counted randomly, and the frequency of morphologically degranulated MCs in 30 mg/kg TPEN-treated ($n = 3$) or nontreated ($n = 3$) mice were calculated. *D*, IgE-dependent PSA was induced, and the plasma histamine concentration was measured after sham ($n = 10$), control ($n = 10$), and 30 mg/kg TPEN ($n = 10$) treatment. Data are representative of three independent experiments, which gave consistent results. The values are the mean ± SEM.

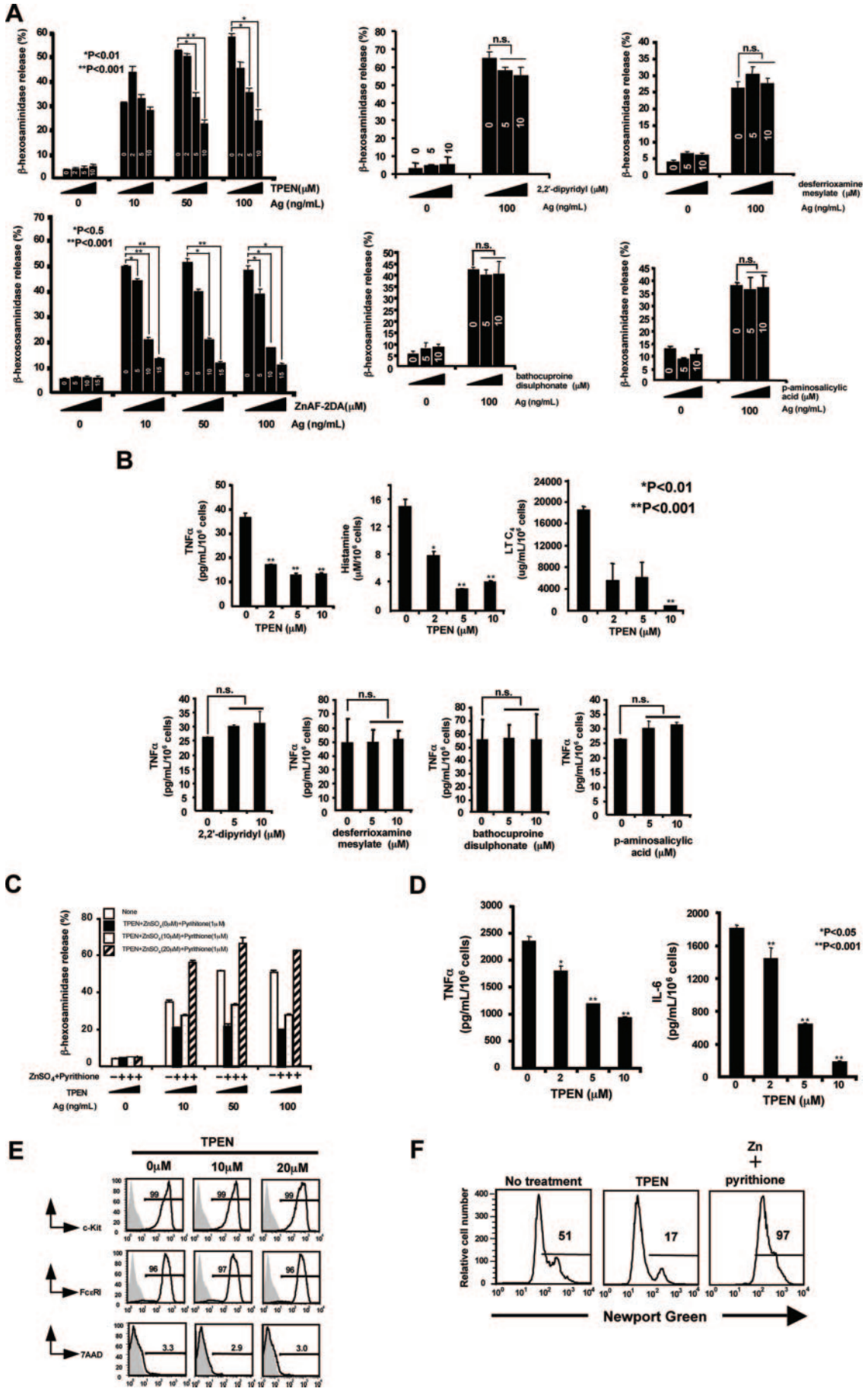

FIGURE 2. (*Figure legend continues*)

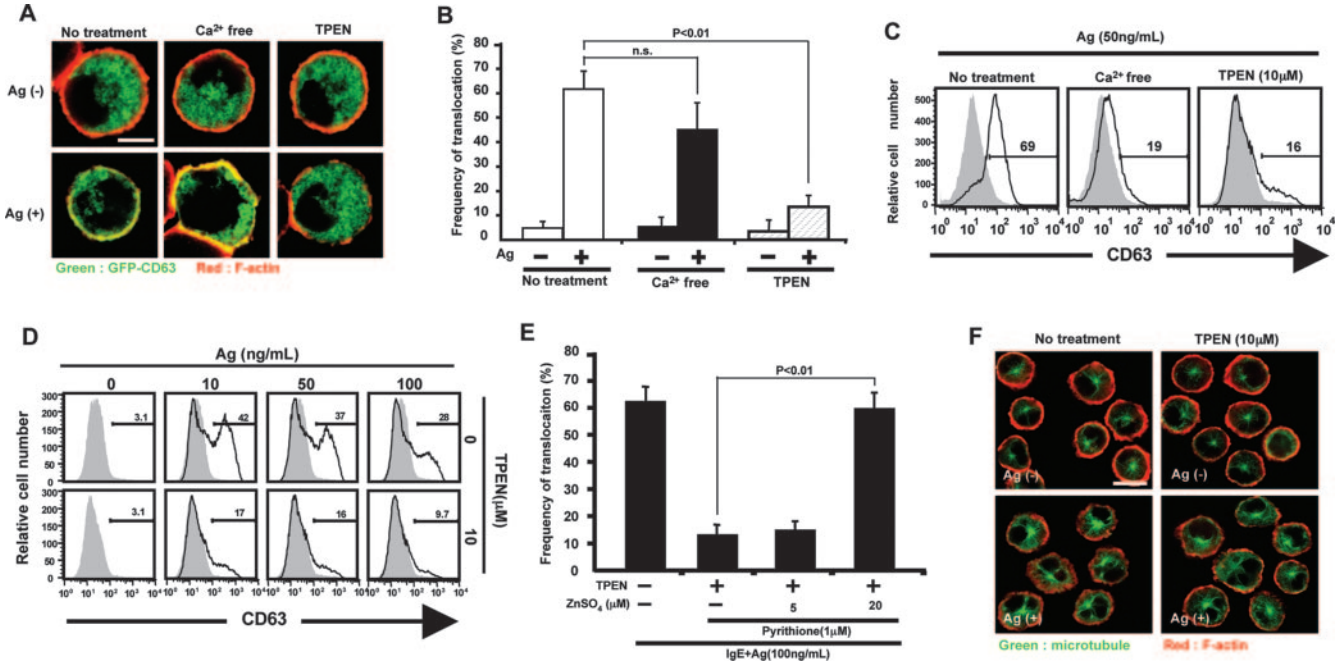

FIGURE 3. Zn chelator inhibits FcεRI-induced granule translocation but not microtubule formation. *A*, BMMCs retrovirally transfected with CD63-GFP were stimulated with Ag for 10 min (0 ng/ml, *upper*; 100 ng/ml, *lower*), and the cells were stained with phalloidin-rhodamine (red) to detect F-actin. Both F-actin and CD63-GFP (green) were visualized by confocal microscopy (*left*, control; *center*, Ca^{2+} free; *right*, TPEN treatment). Scale bar, 5 μm. *B*, The frequency of cells showing granule translocation to the plasma membrane was enumerated as mentioned in the materials and methods. *C*, CD63 expression on the cell surface was detected by FACS. BMMCs were stimulated with Ag in various conditions (*left*, control; *center*, Ca^{2+} free; *right*, TPEN treatment) for 10 min and stained with anti-CD63 after fixation. Gray histograms indicate nonstimulated cells. The percentage of cells in the CD63-positive population is indicated in the figure. *D*, CD63 expression on the cell surface was detected by FACS. BMMCs were stimulated with Ag for 10 min at the concentration indicated under no treatment or 10 μM TPEN treatment and stained with anti-CD63 after fixation. Gray histograms indicate nonstimulated cells. The percentage of cells in the CD63-positive population is indicated in the figure. *E*, The effect of exogenously added Zn^{2+} ion on the granule translocation in TPEN-treated BMMCs. Cells were treated with 10 μM TPEN for 2 h and stimulated with Ag containing the indicated concentrations of $ZnSO_4$, and the frequency of granule-translocated cells was calculated as done in *B*. *F*, Microtubule formation was detected in TPEN-untreated or TPEN-treated cells upon Ag stimulation. BMMCs were stained with phalloidin-rhodamine (red) and FITC-conjugated anti-α-tubulin (green) after stimulation. Scale bar, 10 μm.

reduced in the TPEN-treated mice (Fig. 1*C*, *lower panel*). By microscopic analysis, the total number of ear MCs per field was approximately equal in the TPEN- and sham-treated mice (data not shown). We also assessed the effect of TPEN on Ag-induced histamine release into the blood using a mouse model of PSA. The histamine release was significantly reduced, by 59.1%, in the TPEN-treated mice (Fig. 1*D*). These results clearly show that a Zn chelator effectively inhibited Ag-dependent MC degranulation in vivo.

Zn is required for FcεRI-mediated MC activation.

Because MCs are the major effector cells in PCA and systemic anaphylaxis, we explored the effect of specific Zn chelator, TPEN on BMMC activation. To estimate the extent of Zn depletion caused by TPEN treatment, we performed FACS analysis using impermeable Zn-specific fluorescent indicator, Newport Green, As shown in Fig. 2F, TPEN treatment reduced the level of intracellular Zn in BMMCs. TPEN treatment significantly inhibited the FcεRI-induced β-hexosaminidase, TNF-α, histamine, and leukotriene C_4 release in a concentration-dependent manner (Fig. 2, *A* and *B*). Another Zn chelator, ZnAF-2DA <Ueno, 2002 #65> (30), also inhibited the release of β-hexosaminidase (Fig. 2*A*). However, other metal chelators, such as 2,2′-dipyridyl (for Fe^{2+}), desferrioxamine mesylate (for Fe^{3+}), bathocuproine disulphonate (for Cu^{2+}), and *p*-aminosalicylic acid (for Mn^{2+}) (31–33) did not affect FcεRI-induced MC degranulation (Fig. 2, *A* and *B*). Next, we tested whether inhibitory effect of TPEN is rescued by the addition of $ZnSO_4$. To avoid the use of very high extracellular Zn concentration, which is very cytotoxic, we used a pyrithione, which is an ionophore for Zn, in the rescue experiment (35). The combination of Zn and pyrithione more rapidly increases intracellular Zn levels than by $ZnSO_4$ alone. This inhibitory effect of TPEN was completely

FIGURE 2. FcεRI-dependent MC degranulation and cytokine production were suppressed by Zn chelator. *A*, The effect of Zn chelators and other metal chelators on MC degranulation was assessed. BMMCs were treated with each metal chelator (TPEN and ZnAF-2DA for Zn, 2,2′-dipyridyl and desferrioxamine mesylate for Fe, bathocuproine disulphonate for Cu, and *p*-aminosalicylic acid for Mn) for 2 h, then degranulation after 30 min Ag stimulation was assayed by β-hexosaminidase release. The concentration of each chelator was depicted in the column. *B*, The level of TNF-α, histamine, and leukotriene C_4 released into the culture supernatant after Ag stimulation for 30 min were determined by ELISA. Each chelator was pretreated for 2 h. The values represent the mean $\pm$ SEM ($n = 3$). *C*, BMMCs were untreated or treated with 10 μM TPEN for 2 h, then they were stimulated with Ag containing the indicated concentration of $ZnSO_4$ and 1 μM pyrithione. *D*, Production levels of TNF-α and IL-6 in the cell culture supernatant upon Ag stimulation for 6 h were measured by ELISA. *E*, c-*Kit* and FcεRI expression and cell viability were detected by staining with anti-CD117 (c-*Kit*), anti-IgE, and 7AAD, respectively, in vehicle-, 10, and 20 μM TPEN-treated BMMCs. The term 7AAD-negative means that the cells are viable. *F*, Intracellular Zn contents were detected using Zn indicator, Newport Green. The cells were untreated (*left*), treated with 10 μM TPEN (*center*) and 10 μM $ZnSO_4$ plus 1 μM pyrithione (*right*) as positive control. These experiments were performed at least three times independently, and representative data are shown.

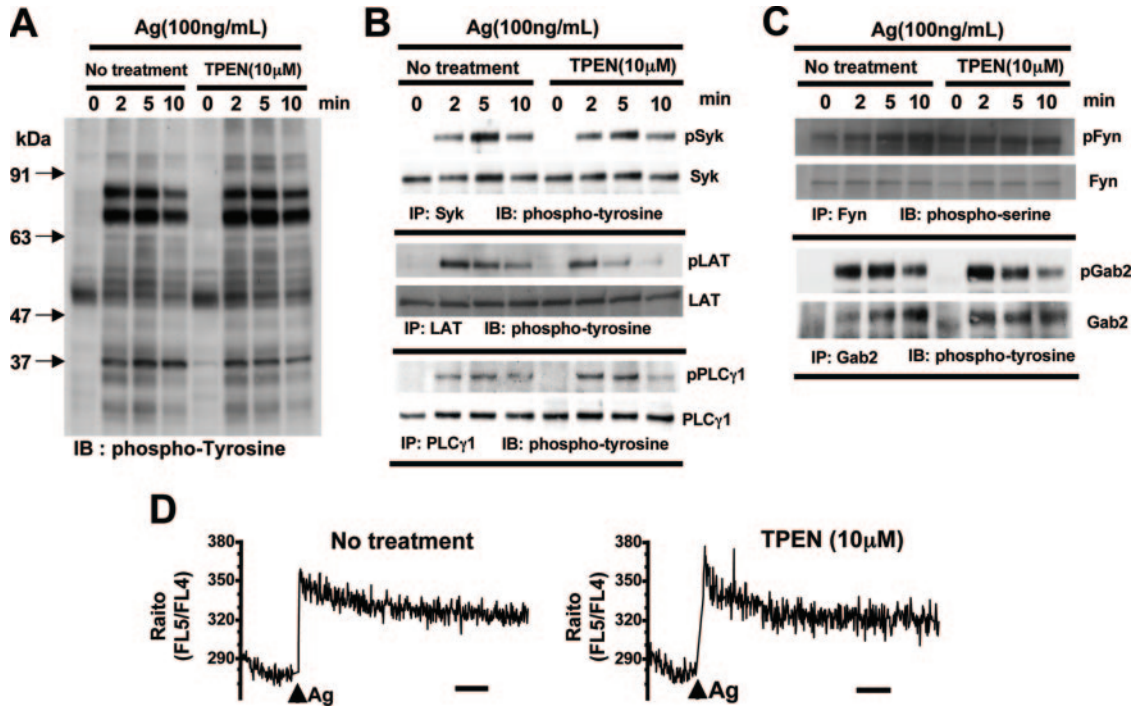

FIGURE 4. Zn chelator does not affect FcεRI-induced global tyrosine phosphorylation or calcium mobilization. *A*, The cells were stimulated with Ag for indicated times with or without TPEN treatment and cell lysates were blotted with anti-phosphotyrosine. *B* and *C*, The effect of TPEN on the activation of molecules involved in FcεRI signal transduction was assessed. Syk, LAT, PLCγ1 and Gab2 were immunoprecipitated with its polyclonal Ab and blotted with phosphotyrosine. For Fyn, immunoprecipitation was performed using anti-Fyn mAb and autotyrosine phosphorylation was detected as mentioned in material and methods. The protein loading was normalized by reprobing the membranes with anti-Syk, anti-LAT, anti- PLCγ1, and anti-Gab2, respectively. *D*, Calcium influx was measured using a calcium-sensitive indicator, indo 1-AM. After incubation with indo 1-AM, cells were stimulated with Ag (100 ng/ml) for 512 s at 37°C. Calcium mobilization is represented as the fluorescence ratio of FL5 (Ca^{2+}-bound indo 1) to FL4 (Ca^{2+}-free indo 1). Bars, 1 min.

rescued by the addition of $ZnSO_4$ (Fig. 2*C*). Taken together, all results indicated that Zn is critically involved in MC degranulation, although we cannot completely neglect the possible involvement of other metals. We also determined the effect of TPEN on cytokine production after 6 h of stimulation. Zn depletion in BMMCs decreased the FcεRI-induced TNF-α and IL-6 production (Fig. 2*D*). Even at the highest TPEN concentration tested (20 μM), the survival and differentiation of BMMCs were not disturbed, in that the TPEN-treated BMMCs were 7-aminoactinomycin D (7AAD)-negative and expressed c-*Kit* and FcεRI on their cell surface at levels similar to those of control BMMCs (Fig. 2*E*).

Zn chelator inhibits FcεRI-induced granule translocation but not microtubule formation.

Recently, we reported that the Fyn/Gab2/RhoA signaling pathway induces granule translocation to the plasma membrane in a manner independent of calcium (18). Therefore, we tested whether Zn is involved in the FcεRI-induced granule translocation process. To visualize the granules, we retrovirally transduced a GFP-CD63 fusion protein expressing plasmids into BMMCs. CD63 is located on the granule membrane in resting MCs (36). Before Ag stimulation, the granule structures were retained in the cytoplasm (Fig. 3*A*). After Ag stimulation, the CD63 signal was observed near the plasma membrane by confocal microscopy (Fig. 3A), and detected on the cell surface by FACS (Fig. 3*C*, *left panel*), suggesting that the granules were translocated from the cytoplasm to the plasma membrane, and that granule-plasma membrane fusion had occurred. In calcium-free medium, in which degranulation is completely abolished, no increased cell surface expression of CD63 was detected by FACS (Fig. 3*C*, *center panel*), while the granule translocation to the plasma membrane was still detected by confocal microscopy as we previously showed (Fig. 3*A*, *center panel*, and *B*) (18). Notably, treatment with TPEN significantly suppressed the FcεRI-induced granule translocation to the plasma membrane detected by confocal microscopy (Fig. 3*A*, *right panel*, and *B*) as well as the Ag-induced cell surface expression of CD63 (Fig. 3*C*, *right panel*, and *D*). Furthermore, we confirmed that reloading with Zn rescued the defect in FcεRI-induced granule translocation in Zn-depleted BMMCs (Fig. 3*E*). These results show that Zn was essential for the calcium-independent process of granule translocation to the plasma membrane. Because granule translocation is dependent on microtubules (18, 37), we next investigated whether Zn-depletion inhibited FcεRI-induced microtubule formation. As a result, TPEN treatment had no effect on microtubule formation upon Ag stimulation, while granules did not move to the plasma membrane in TPEN-treated BMMCs. (Fig. 3*F* and data not shown). The above results suggested that Zn chelator could be effective for interfering with FcεRI-mediated granule translocation in MCs.

Zn chelator does not affect FcεRI-induced global tyrosine phosphorylation or calcium mobilization.

FcεRI-induced signaling in MCs involves the tyrosine phosphorylation of various signaling molecules and calcium influx, both of which are critical for MC degranulation. We next monitored the effect of TPEN on these FcεRI-induced signaling events. In TPEN-treated BMMCs the total cellular, Syk, Fyn, LAT, Gab2, and PLCγ1 tyrosine phosphorylation was apparently normal, although the phosphorylation of LAT and PLCγ1 appeared to be more transient and the intensity of phosphorylation of the protein bands above the 91-kDa marker appear to be intensified (Fig. 4, *A–C*). The FcεRI-induced calcium influx was also apparently normal in TPEN-treated BMMCs (Fig. 4*D*). These results suggest that

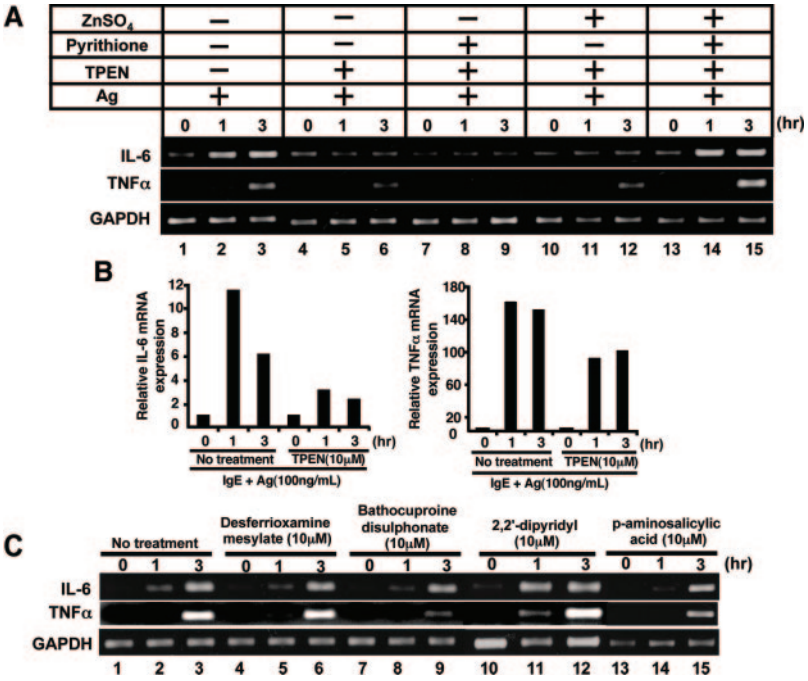

FIGURE 5. IL-6 and TNF-α gene expression induced by Ag stimulation was suppressed by Zn chelator, but not with other metal chelators. *A*, The cells were stimulate for 0, 1, and 3 h under various conditions, then IL-6 and TNF-α gene expression levels were analyzed for RT-PCR. *Lanes 1–3*; no treatment, *lanes 4–6*; 10 μM TPEN, *lanes 7–9*; 10 μM TPEN plus 0.1 μM pyrithione, *lanes 10–12*; 10 μM TPEN plus 10 μM $ZnSO_4$, *lanes 13–15*; 10 μM TPEN plus 0.1 μM pyrithione plus 10 μM $ZnSO_4$. *B*, IL-6 and TNF-α expressions at mRNA level were assessed by real-time quantitative RT-PCR. BMMCs were untreated or treated with 10 μM TPEN for 2 h and stimulated with Ag for indicated times. *C*, IL-6 and TNF-α expressions at mRNA level were assessed by RT-PCR as in (*A*). The cells were pretreated with indicated concentration of metal chelators as used in Fig. 2*A*. These experiments were performed at least three times independently, and representative data are shown.

there is an action point of TPEN besides tyrosine phosphorylation and calcium-elicited signaling.

Zn chelator inhibits FcεRI-induced NF-κB activation.

To define the molecular mechanism(s) responsible for the defective cytokine production in Zn-depleted BMMCs, we analyzed cytokine mRNA levels using RT-PCR. FcεRI stimulation of BMMCs led to an increase in IL-6 and TNF-α mRNA level in a time-dependent manner. However, Zn-depleted BMMCs decreased IL-6 and TNF-α mRNA level (Fig. 5, *A* and *B*). This inhibitory effect of TPEN was rescued by the addition of $ZnSO_4$ (Fig. 5*A*). Furthermore, other metal chelators did not affect IL-6 and TNF-α mRNA level (Fig. 5*C*). Thus, Zn is involved in FcεRI-induced IL-6 and TNF-α gene transcription, in particular IL-6. In general, the transcription of IL-6 and TNF-α was regulated by a transcription factor, NF-κB. NF-κB consists of p65 and p50 heterodimer and retained in cytoplasm by binding with IκBα in resting state. NF-κB nuclear translocation was occurred after IκBα serine phosphorylation by IκB kinase $\alpha\beta$ (IKK$\alpha\beta$), leading to the degradation of IκBα (38). We analyzed whether TPEN inhibited

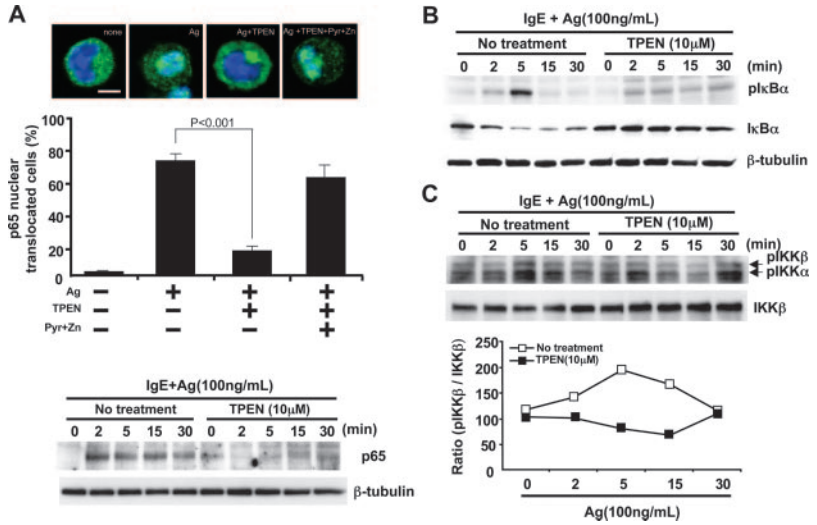

FIGURE 6. NF-κB activation pathway induced by Ag stimulation is inhibited by Zn chelator pretreatment. BMMCs were untreated or treated with 10 μM TPEN for 2 h and stimulated for indicated times. *A*, NF-κB nuclear translocation was visualized by confocal microscopy. After Ag or Ag with 1 μM pyrithione plus 10 μM $ZnSO_4$ stimulation, cells were stained with anti-p65, FITC-conjugated anti-rabbit Ab and 4′, 6-diamidino-2-phenylindole dihydrochloride. Green indicates p65, and blue indicates nucleus. Scale bar, 5 μm. A total of 50 cells were counted randomly in each sample, and the frequency of NF-κB nuclear-translocated cells was calculated. The values are the mean ± SEM. (*Bottom*) Western blot analysis was performed on nuclear extracts to assess the effect of TPEN of NF-κB nuclear translocation. Nuclear extraction was blotted with anti-p65 Ab. Protein loading was normalized by reprobing the membrane with anti-β tubulin. *B* and *C*, IκBα phosphorylation, degradation, and IKK$\alpha\beta$ phosphorylation were determined. After Ag stimulation, cells were lysed and cytosol faraction was immunoblotted with anti-phospho-IkBα and anti-phospho-IKK$\alpha\beta$, respectively. Protein loading was normalized by reprobing the membrane with anti-IkBα and anti-IKK$\alpha\beta$, respectively. As for IKK$\alpha\beta$, the extent of serine phosphorylation was densitometrically enumerated normalized by densitometry of IKKβ.

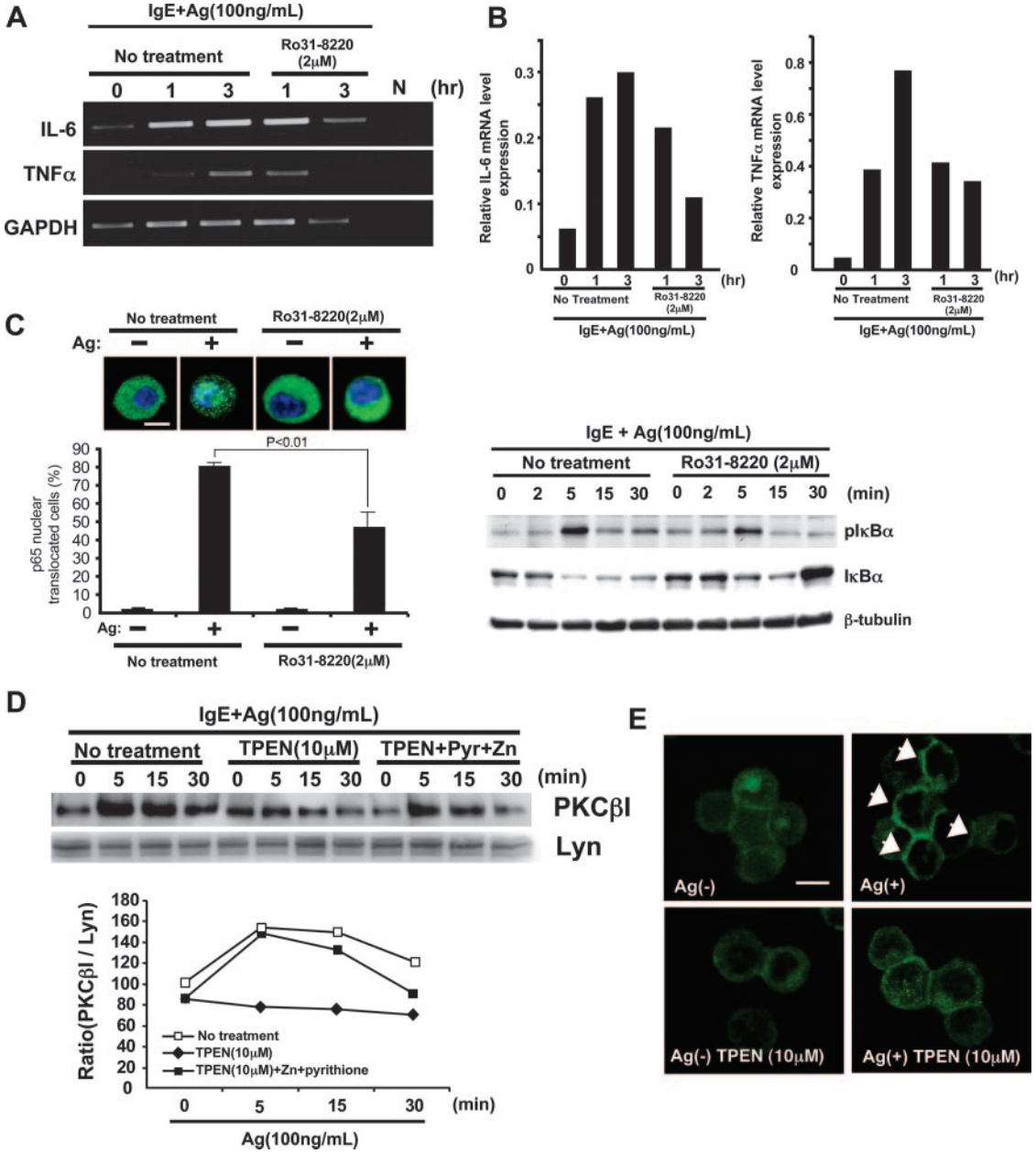

FIGURE 7. PKC is involved in Ag-induced IL-6 and TNF-α mRNA expression, and plasma membrane translocation of PKC was inhibited by Zn chelator. To assess the involvement of PKC on Ag-induced IL-6 and TNF-α gene expression, cells were treated with 2 μM PKC family inhibitor, Ro31-8220, at the same time as Ag stimulation and total RNA was extracted after Ag stimulation for 1 and 3 h. Total RNA (1 μg) was used for reverse transcription. mRNA (50 ng) was analyzed for IL-6 and TNF-α expression level by RT-PCR (*A*) and by real-time quantitative RT-PCR (*B*). *C*, NF-κB nuclear translocation was visualized by confocal microscopy. After Ag stimulation, cells were stained with anti-p65, FITC-conjugated anti-rabbit Ab and 6-diamidino-2-phenylindole dihydrochloride. Green indicates p65 and blue indicated nucleus. Scale bar, 5 μm. The frequency of NF-κB nuclear-translocated cells was calculated as in Fig. 6*A*. The values are the mean $\pm$ SEM. Phosphorylation of IκBα and degradation of IκBα in the cytosol fraction were detected by immunobloting after Ag stimulation under the treatment with or without 2 μM Ro31-8220. *D*, After Ag stimulation for indicated time in the presence or absence of 10 μM TPEN, cells were lysed, plasma membrane fraction was extracted, and PKCβI was detected by immunoblot. The protein loading was normalized by reprobing the membranes with anti-Lyn Ab. PKC plasma membrane translocation was densitometrycally enumerated in a bottom panel. *E*, PKCβI plasma membrane translocation was visualized by confocal microscopy. Cells were either untreated or treated with 10 μM TPEN for 2 h and stimulated with Ag for 10 min. After Ag stimulation, cells were fixed and stained with polyclonal anti-PKCβI Ab. Arrows indicate PKCβI. These experiments were performed at least three times independently, and representative data are shown.

FcεRI-induced nuclear translocation of p65. The cells were stained with anti-p65 after stimulation under the TPEN treatment. As a result, Zn-depleted BMMCs significantly reduced FcεRI-induced translocation of p65 to the nucleus (Fig. 6*A*). Furthermore, we confirmed that this inhibitory effect of TPEN was rescued by the addition of $ZnSO_4$ (Fig. 6*A*), indicating that Zn is essential for nuclear translocation of NF-κB in MCs. Consistent with these results, FcεRI-mediated IκBα phosphorylation and its subsequent degradation were impaired in Zn-depleted BMMCs (Fig. 6*B*). Finally, we examined the effect of Zn depletion on the activation of IKKα and IKKβ, which regulate IκBα phosphorylation. As shown in Fig. 6*C*, TPEN inhibited FcεRI-induced IKKβ phosphorylation. Together, these results showed that Zn-dependent mechanism is required for FcεRI-mediated NF-κB activation pathway.

Zn is involved in FcεRI-induced plasma membrane translocation of PKCβ I.

Because IκBα phosphorylation through IKKβ was decreased in Zn-depleted BMMCs as described in Fig. 6, we next investigated the upstream target of Zn involved in NF-κB activation. Because recent studies demonstrated a role for PKC-mediated signals in the control of NF-κB activation (39–41), we examined whether PKC is involved in FcεRI-mediated NF-κB activation in MCs. As shown in Fig. 7, *A* and *B*, PKC inhibitor, Ro31–8220 inhibited FcεRI-induced up-regulation of IL-6 and TNF-α mRNA. Consistent with this result, FcεRI-induced NF-κB nuclear translocation, IκBα phosphorylation, and IκBα degradation were partially blocked by Ro31-8220 treatment (Fig. 7*C*). Based on known function of PKC, we hypothesized that Zn is required for NF-κB activation because it is required for PKC activation in MCs. To test this hypothesis, we examined the effect of TPEN plasma membrane translocation of PKC, a process important for PKC function (42, 43). As shown in Fig. 7, *D* and *E*, FcεRI-induced plasma membrane translocation of PKCβI was inhibited in Zn-depleted BMMCs.

Discussion

In this study, we showed that the Zn chelator TPEN inhibited the IgE-dependent PCA and systemic anaphylaxis reactions. Consistent with this in vivo effect, the Zn chelator strongly inhibited the FcεRI-induced degranulation (i.e., histamine and β-hexosaminidase release) in vitro. Furthermore, it inhibited the FcεRI-mediated cytokine production and leukotriene release, indicating that Zn-dependent mechanisms are involved in MC activation. We also showed that the reloading of Zn could rescue the degranulation defect in Zn-depleted BMMCs, indicating that the effect of the Zn chelator is a reversible reaction. In the 1960s, electron microscopic studies demonstrated that MCs are rich in heavy metals such as Zn and Fe, but not Cu (3). Because TPEN has affinities for other heavy metals, we checked other metal chelators such as 2,2′-dipyridyl (for Fe^{2+}), desferrioxamine mesylate (for Fe^{3+}), bathocuproine disulphonate (for Cu^{2+}), and *p*-aminosalicylic acid (for Mn^{2+}) on degranulation and cytokine induction. These metal chelators treatment did not affect FcεRI-induced MC degranulation and cytokine induction. Because the inhibitory effect of TPEN was suppressed by the treatment with Zn and ionophore, all results are consistent with the notion that Zn is involved in MC degranulation process and cytokine production, although we cannot dismiss the possible involvement of other metals.

How might the Zn chelator exert its inhibitory effect? We confirmed that it had no effect on the early FcεRI-induced tyrosine phosphrylation of a variety of signaling molecules or on calcium mobilization, but it strongly suppressed the FcεRI-induced granule translocation. Vesicle transport generally depends on cytoskeletal proteins such as tubulin and actin (44). In MCs, several reports including ours have shown that microtubules are important for FcεRI-induced degranulation and granule translocation to the plasma membrane (18, 37, 45). However, in this study, we showed that TPEN had no effect on FcεRI-induced microtubule formation. This result may suggest the existence of a molecule linking microtubules and granules. Recently, kinesin receptors, or linker-cargo proteins, were identified (46). These molecules have a kinesin-interacting region and link kinesin to vesicles. One target of TPEN may be such a linker molecule-one with a Zn finger or Zn-binding domain. In addition to the granule translocation, TPEN might control the process of granule-membrane fusion through Rab-effector molecules because several groups have reported that Rab-effector molecules such as Rim, Granulophilin, and Rabphilin regulate fusion of synaptic vesicle and have Zn-finger domain (47, 48). In addition, PKC may be involved in granule translocation process as discussed later.

In this study, we also showed that Zn chelator suppressed FcεRI-mediated cytokine production and transcription of IL-6 and TNF-α mRNA. Importantly, this inhibitory effect could be rescued by addition of $ZnSO_4$, suggesting that Zn is essential for FcεRI-mediated cytokine gene expression. Previously, it was reported that PKC is activated with Ag stimulation and involved in cytokine production in MCs and that Zn-binding domain of PKC is required for plasma membrane translocation after stimulation (24, 25). These observations may suggest Zn plays a role in the regulation of PKC plasma membrane translocation. In fact, in this study, we showed that TPEN inhibited plasma membrane translocation of PKCβI using biochemical and microscopic approaches. These results suggested that one of targets of TPEN involved in cytokine production was PKC. In addition to PKC, TPEN treatment strongly inhibited IκBα phosphorylation and its degradation. Accordingly, p65 nuclear translocation was significantly inhibited by TPEN treatment. These results indicate that modification of Zn level by TPEN can affect NF-κB activation pathway. Recently, it was reported that PKC was involved in NF-κB activation pathway in MCs by using Ro31-8220, a pharmaceutical inhibitor of PKC (49). Consistent with this reports, Ro31-8220 partially inhibited IκBα phosphorylation and its degradation. These results suggest that suppression of cytokine production by TPEN is partly due to inactivation of PKCβI/NF-κB activation pathway. Furthermore, PKC may contribute to FcεRI-mediated granule translocation, because PKC family molecules have multiple effects for regulation of exocytosis and endocytosis (50). Thus, PKC might be one of target molecules of TPEN in MCs. However, we also consider that there exist some other targets of TPEN. TPEN might control the process of protein degradation through inhibiting ubiquitination. Because E3 ligases which play a pivotal role in ubiquitination have the catalytic domain containing a Zn-binding RING finger motif (51). TPEN might suppress E3 ligase activity to inhibit IκBα degradation. Mutational analyses of these candidates molecules, such as PKC and E3 ligases will be required to clarify these points.

In summary, Zn is essential for FcεRI-mediated MC activation (i.e., degranulation and cytokine production). Our data indicate the presence of multiple Zn-dependent mechanisms in MC activation. These findings strongly suggest that Zn chelator is a promising new drug that acts differently from other antiallergic drugs such as histamine antagonists. We postulate that controlling the concentration of Zn in MCs may become a useful strategy for developing novel anti-allergy treatments.

Acknowledgments

We thank Drs. M. Nakanishi, K. Hattori, G. Nolan, and T. Kitamura for various reagents; and Drs. E. Morii and K. Oboki for technical advice and suggestions. We also thank M. Kikuchi for excellent technical assistance and M. Shimura for secretarial assistance.

Disclosures

The authors have no financial conflict of interest.

References

1. Prasad, A. S. 1998. Zinc and immunity. *Mol. Cell. Biochem.* 188: 63–69.
2. Koh, J. Y. 2001. Zinc and disease of the brain. *Mol. Neurobiol.* 24: 99–106.
3. Gustafson, G. T. 1967. Heavy metals in rat mast cell granules. *Lab. Invest.* 17: 588–598.
4. Wedemeyer, J., M. Tsai, and S. J. Galli. 2000. Roles of mast cells and basophils in innate and acquired immunity. *Curr. Opin. Immunol.* 12: 624–631.
5. Galli, S. J., and S. Nakae. 2003. Mast cells to the defense. *Nat. Immunol.* 4: 1160–1162.

6. Galli, S. J., J. Kalesnikoff, M. A. Grimbaldeston, A. M. Piliponsky, C. M. Williams, and M. Tsai. 2005. Mast cells as "tunable" effector and immunoregulatory cells: recent advances. *Annu. Rev. Immunol.* 23: 749–786.
7. Rottem, M., and Y. A. Mekori. 2005. Mast cells and autoimmunity. *Autoimmun. Rev.* 4: 21–27.
8. Galli, S. J. 1993. New concepts about the mast cell. *N. Engl. J. Med.* 328: 257–265.
9. Williams, C. M., and S. J. Galli. 2000. The diverse potential effector and immunoregulatory roles of mast cells in allergic disease. *J. Allergy Clin. Immunol.* 105: 847–859.
10. Kinet, J. P. 1999. The high-affinity IgE receptor (FcεRI): from physiology to pathology. *Annu. Rev. Immunol.* 17: 931–972.
11. Metcalfe, D. D., D. Baram, and Y. A. Mekori. 1997. Mast cells. *Physiol. Rev.* 77: 1033–1079.
12. Turner, H., and J. P. Kinet. 1999. Signalling through the high-affinity IgE receptor FcεRI. *Nature* 402: B24–B30.
13. Rivera, J. 2002. Molecular adapters in FcεRI signaling and the allergic response. *Curr. Opin. Immunol.* 14: 688–693.
14. Blank, U., and J. Rivera. 2004. The ins and outs of IgE-dependent mast-cell exocytosis. *Trends Immunol.* 25: 266–273.
15. Kawakami, T., and S. J. Galli. 2002. Regulation of mast-cell and basophil function and survival by IgE. *Nat. Rev. Immunol.* 2: 773–786.
16. Guo, Z., C. Turner, and D. Castle. 1998. Relocation of the t-SNARE SNAP-23 from lamellipodia-like cell surface projections regulates compound exocytosis in mast cells. *Cell* 94: 537–548.
17. Castle, J. D., Z. Guo, and L. Liu. 2002. Function of the t-SNARE SNAP-23 and secretory carrier membrane proteins (SCAMPs) in exocytosis in mast cells. *Mol. Immunol.* 38: 1337–1340.
18. Nishida, K., S. Yamasaki, Y. Ito, K. Kabu, K. Hattori, T. Tezuka, H. Nishizumi, D. Kitamura, R. Goitsuka, R. S. Geha, et al. 2005. FcεRI-mediated mast cell degranulation requires calcium-independent microtubule-dependent translocation of granules to the plasma membrane. *J. Cell Biol.* 170: 115–126.
19. Gordon, J. R., and S. J. Galli. 1990. Mast cells as a source of both preformed and immunologically inducible TNF-α/cachectin. *Nature* 346: 274–276.
20. Gordon, J. R., P. R. Burd, and S. J. Galli. 1990. Mast cells as a source of multifunctional cytokines. *Immunol. Today* 11: 458–464.
21. Baumgartner, R. A., K. Yamada, V. A. Deramo, and M. A. Beaven. 1994. Secretion of TNF from a rat mast cell line is a brefeldin A-sensitive and a calcium/protein kinase C-regulated process. *J. Immunol.* 153: 2609–2617.
22. Chang, E. Y., Z. Szallasi, P. Acs, V. Raizada, P. C. Wolfe, C. Fewtrell, P. M. Blumberg, and J. Rivera. 1997. Functional effects of overexpression of protein kinase C-α, -β, -δ, -ε, and -η in the mast cell line RBL-2H3. *J. Immunol.* 159: 2624–2632.
23. Ono, Y., T. Fujii, K. Igarashi, T. Kuno, C. Tanaka, U. Kikkawa, and Y. Nishizuka. 1989. Phorbol ester binding to protein kinase C requires a cysteine-rich zinc-finger-like sequence. *Proc. Natl. Acad. Sci. USA* 86: 4868–4871.
24. Sakai, N., K. Sasaki, N. Ikegaki, Y. Shirai, Y. Ono, and N. Saito. 1997. Direct visualization of the translocation of the γ-subspecies of protein kinase C in living cells using fusion proteins with green fluorescent protein. *J. Cell Biol.* 139: 1465–1476.
25. Oancea, E., M. N. Teruel, A. F. Quest, and T. Meyer. 1998. Green fluorescent protein (GFP)-tagged cysteine-rich domains from protein kinase C as fluorescent indicators for diacylglycerol signaling in living cells. *J. Cell Biol.* 140: 485–498.
26. Nechushtan, H., M. Leitges, C. Cohen, G. Kay, and E. Razin. 2000. Inhibition of degranulation and interleukin-6 production in mast cells derived from mice deficient in protein kinase Cβ. *Blood* 95: 1752–1757.
27. Arslan, P., F. Di Virgilio, M. Beltrame, R. Y. Tsien, and T. Pozzan. 1985. Cytosolic $Ca2^+$ homeostasis in Ehrlich and Yoshida carcinomas: a new, membrane-permeant chelator of heavy metals reveals that these ascites tumor cell lines have normal cytosolic free $Ca2^+$. *J. Biol. Chem.* 260: 2719–2727.
28. McCabe, M. J., Jr., S. A. Jiang, and S. Orrenius. 1993. Chelation of intracellular zinc triggers apoptosis in mature thymocytes. *Lab. Invest.* 69: 101–110.
29. Ueno, S., M. Tsukamoto, T. Hirano, K. Kikuchi, M. K. Yamada, N. Nishiyama, T. Nagano, N. Matsuki, and Y. Ikegaya. 2002. Mossy fiber $Zn2^+$ spillover modulates heterosynaptic *N*-methyl-*D*-aspartate receptor activity in hippocampal CA3 circuits. *J. Cell Biol.* 158: 215–220.
30. Hirano, T., K. Kikuchi, Y. Urano, and T. Nagano. 2002. Improvement and biological applications of fluorescent probes for zinc, ZnAFs. *J. Am. Chem. Soc.* 124: 6555–6562.
31. Armstrong, C., W. Leong, and G. J. Lees. 2001. Comparative effects of metal chelating agents on the neuronal cytotoxicity induced by copper (Cu^{2+}), iron (Fe^{3+}) and zinc in the hippocampus. *Brain Res.* 892: 51–62.
32. Tandon, S. K., and J. Singh. 1975. Removal of manganese by chelating agents from brain and liver of manganese treated rats: as in vitro and an in vivo study. *Toxicology.* 5: 237–241.
33. Ky, S. Q., H. S. Deng, P. Y. Xie, and W. Hu. 1992. A report of two cases of chronic serious manganese poisoning treated with sodium para-aminosalicylic acid. *Br. J. Ind. Med.* 49: 66–69.
34. Nishida, K., L. Wang, E. Morii, S. J. Park, M. Narimatsu, S. Itoh, S. Yamasaki, M. Fujishima, K. Ishihara, M. Hibi, et al. 2002. Requirement of Gab2 for mast cell development and KitL/c-*Kit* signaling. *Blood* 99: 1866–1869.
35. Dineley, K. E., J. M. Scanlon, G. J. Kress, A. K. Stout, and I. J. Reynolds. 2000. Astrocytes are more resistant than neurons to the cytotoxic effects of increased (Zn^{2+})(i). *Neurobiol. Dis.* 7: 310–320.
36. Nishikata, H., C. Oliver, S. E. Mergenhagen, and R. P. Siraganian. 1992. The rat mast cell antigen AD1 (homologue to human CD63 or melanoma antigen ME491) is expressed in other cells in culture. *J. Immunol.* 149: 862–870.
37. Smith, A. J., J. R. Pfeiffer, J. Zhang, A. M. Martinez, G. M. Griffiths, and B. S. Wilson. 2003. Microtubule-dependent transport of secretory vesicles in RBL-2H3 cells. *Traffic* 4: 302–312.
38. Karin, M., and Y. Ben-Neriah. 2000. Phosphorylation meets ubiquitination: the control of NF-κB activity. *Annu. Rev. Immunol.* 18: 621–663.
39. Sun, Z., C. W. Arendt, W. Ellmeier, E. M. Schaeffer, M. J. Sunshine, L. Gandhi, J. Annes, D. Petrzilka, A. Kupfer, P. L. Schwartzberg, and D. R. Littman. 2000. PKC-θ is required for TCR-induced NF-κB activation in mature but not immature T lymphocytes. *Nature* 404: 402–407.
40. Su, T. T., B. Guo, Y. Kawakami, K. Sommer, K. Chae, L. A. Humphries, R. M. Kato, S. Kang, L. Patrone, R. Wall, et al. 2002. PKC-β controls IκB kinase lipid raft recruitment and activation in response to BCR signaling. *Nat. Immunol.* 3: 780–786.
41. Weil, R., and A. Israel. 2004. T-cell-receptor- and B-cell-receptor-mediated activation of NF-κB in lymphocytes. *Curr. Opin. Immunol.* 16: 374–381.
42. Khoshnan, A., D. Bae, C. A. Tindell, and A. E. Nel. 2000. The physical association of protein kinase C-θ with a lipid raft-associated inhibitor of κB factor kinase (IKK) complex plays a role in the activation of the NF-κB cascade by TCR and CD28. *J. Immunol.* 165: 6933–6940.
43. Bi, K., Y. Tanaka, N. Coudronniere, K. Sugie, S. Hong, M. J. van Stipdonk, and A. Altman. 2001. Antigen-induced translocation of PKC-theta to membrane rafts is required for T cell activation. *Nat. Immunol.* 2: 556–563.
44. Goode, B. L., D. G. Drubin, and G. Barnes. 2000. Functional cooperation between the microtubule and actin cytoskeletons. *Curr. Opin. Cell Biol.* 12: 63–71.
45. Martin-Verdeaux, S., I. Pombo, B. Iannascoli, M. Roa, N. Varin-Blank, J. Rivera, and U. Blank. 2003. Evidence of a role for Munc18–2 and microtubules in mast cell granule exocytosis. *J. Cell Sci.* 116: 325–334.
46. Schnapp, B. J. 2003. Trafficking of signaling modules by kinesin motors. *J. Cell Sci.* 116: 2125–2135.
47. Chung, S. H., Y. Takai, and R. W. Holz. 1995. Evidence that the Rab3a-binding protein, rabphilin3a, enhances regulated secretion. Studies in adrenal chromaffin cells. *J. Biol. Chem.* 270: 16714–16718.
48. Sudhof, T. C. 2004. The synaptic vesicle cycle. *Annu. Rev. Neurosci.* 27: 509–547.
49. Peng, Y., M. R. Power, B. Li, and T. J. Lin. 2005. Inhibition of IKK downregulates antigen + IgE-induced TNF production by mast cells: a role for the IKK-IκB-NF-κB pathway in IgE-dependent mast cell activation. *J. Leukocyte. Biol.* 77: 975–983.
50. Ozawa, K., Z. Szallasi, M. G. Kazanietz, P. M. Blumberg, H. Mischak, J. F. Mushinski, and M. A. Beaven. 1993. $Ca(^{2+})$-dependent and $Ca(^{2+})$-independent isozymes of protein kinase C mediate exocytosis in antigen-stimulated rat basophilic RBL-2H3 cells. Reconstitution of secretory responses with Ca^{2+} and purified isozymes in washed permeabilized cells. *J. Biol. Chem.* 268: 1749–1756.
51. Liu, Y. C. 2004. Ubiquitin ligases and the immune response. *Annu. Rev. Immunol.* 22: 81–127.